Desalination and Water Treatment
www.deswater.com
doi: 10.5004/dwt.2019.24653

168 (2019) 269–281
November

Preparation of bamboo-based oxidized biochar for simultaneous removal of Cd(II) and Cr(VI) from aqueous solutions

Bei Chu[a,*], Yoshimasa Amano[b,c], Motoi Machida[b,c]

[a]*Graduate School of Science and Engineering, Chiba University, Yayoi-cho 1-33, Inage-ku, Chiba 263-8522, Japan, email: chubei@chiba-u.jp*
[b]*Graduate School of Engineering, Chiba University, Yayoi-cho 1-33, Inage-ku, Chiba 263-8522, Japan,*
emails: amanoy@faculty.chiba-u.jp (Y. Amano), machida@faculty.chiba-u.jp (M. Machida)
[c]*Safety and Health Organization, Chiba University, Yayoi-cho 1-33, Inage-ku, Chiba 263-8522, Japan*

Received 13 March 2019; Accepted 29 June 2019

ABSTRACT

Cd(II) and Cr(VI) are highly toxic heavy metal ions, which commonly coexist in industrial wastewater. In this study, simultaneous removal of Cd(II) and Cr(VI) by a bamboo-based oxidized biochar (BZ-APS24h) was investigated. The biochar was modified by $ZnCl_2$ and oxidized with $(NH_4)_2S_2O_8$, and its structures as characterized by SEM, BET, elemental composition and X-ray photoelectron spectroscopy. Batch adsorption experiments for Cd(II) and Cr(VI) were carried out to explore the effects of oxidation time, pH, contact time, temperature and coexisting ions on its adsorption process. The results showed that the BZ-APS24h exhibited excellent adsorption performance for the removal of Cd(II) (0.27 mmol/g) and Cr(VI) (0.65 mmol/g). The adsorption data were fitted well with pseudo-second-order model and Langmuir isotherm. The pH of the solution had a great influence on the adsorption process. The coexistence of Cd(II) and Cr(VI) affected the equilibrium pH after adsorption, and synergistic adsorption was also observed.

Keywords: Bamboo; Oxidized biochar; Simultaneous removal; Cd(II); Cr(VI)

1. Introduction

With the rapid development of industry, more and more industrial wastewater has been discharged into the environment directly. Cd(II) and Cr(VI) are the common highly toxic heavy metals, which widely exist in printing and dyeing wastewater, electroplating wastewater and other industrial wastewater [1,2]. Cadmium has adverse effects on human health, including pulmonary insufficiency, renal dysfunction, cancer, disease and hypertension [3]. Cadmium exists in water mainly in the main form of Cd(II) (Cd^{2+}). Unlike cadmium, the main forms of chromium in aqueous solution are Cr(III) (Cr^{3+}, $Cr(OH)_2^+$) and Cr(VI) ($HCrO_4^-$, CrO_4^{2-}, $Cr_2O_7^{2-}$) [4,5], and Cr(VI) is approximately 100 times highly toxic than Cr(III) [6]. Cr(VI) is easily adsorbed by the human body, and has a great toxicity to human kidney, stomach and liver [7]. Cd(II) and Cr(VI) ions are both extremely toxic metals that usually exist simultaneously in electroplating, paint pigmentations, and printing and dyeing, and wastewater [8,9]. The co-occurring pollutants exhibit complicated interactions in adsorption behaviors [10]. Thus it is important to remove these heavy metals before discharging into environment.

Existing methods for removal of Cr(VI) and Cd(II) from water include chemical precipitation [11,12], membrane filtration [13,14], ion exchange [15,16], adsorption [17] and biological processes [18,19]. Adsorption method is known to be an easy, low cost and high efficiency method for the treatment of heavy metals such as Cd(II) and Cr(VI) [20]. Surface adsorption is mainly dominated by electrostatic interaction, hydrogen bonding, π-π stacking and pore-filling [21]. In the

* Corresponding author.

adsorption method, the selection of adsorbent is decisively important. Widely-used adsorbents such as biochar, zeolites, and molecular sieves generally have a large specific surface area. Among them, biochar derived from biomass has been proved to be a universal adsorbent for heavy metal because of its favorable physicochemical properties and relatively low cost [22–24]. Moso bamboo is abundant, especially in Asia. It is characterized by the rapid growth (getting mature within 3–5 years only) compared with other plants, and thus is regarded as cheaply available biochar material [25].

However, most of the biochar have low surface area due to the lack of porous structure. In order to overcome this shortcoming, $ZnCl_2$ is generally used as a surface active agent to increase the specific surface area and the adsorption ability of biochar [26]. The higher specific surface area also allows the biochar surface to have a higher positive charge, which facilitates the adsorption of various anions (e.g., $Cr_2O_7^{2-}$, CrO_4^{2-}, NO_3^- and PO_4^{2-}) [27]. Biochar not only has a porous structure but also has some oxygen-containing functional groups on its surface. These oxygen-containing functional groups provide a prevalence of negative charges on the biochar which have the ability to adsorb cations (e.g., Cu^{2+}, Cd^{2+}, Pb^{2+} and Ni^{2+}) [28]. Although the surface of biochar contains a certain amount of oxygen-containing functional groups, the number of the functional groups is small. Therefore, the oxygen-containing functional groups can be introduced to the surface of the biochar by oxidation method [29].

At present, there are many studies on the adsorption of Cd(II) or Cr(VI) by biochar [30,31], but these biochar were commonly used to remove Cd(II) or Cr(VI) separately rather than simultaneously [32]. Because the adsorption potentials of Cd(II) and Cr(VI) are different, this becomes the main factor restricting their simultaneous adsorption. In previous studies, simultaneous removal of Pb(II) and Cr(VI) by a novel sewage sludge-derived biochar immobilized nanoscale zero-valent iron (SSB-nZVI) was reported [33]. However, the change of pH in the process of adsorption is often neglected. Furthermore, the presence of one metal ion in the solution may affect the adsorption of another metal ion. Hence, it is crucial to study the interaction of two ions in adsorption.

In this work, Cd(II) and Cr(VI) were selected as two representative heavy metals. The bamboo-based biochar was prepared, which was then modified by $ZnCl_2$ and oxidized by $(NH_4)_2S_2O_8$ solution for the removal of Cd(II) and Cr(VI). The main objectives of this paper are: (1) to assess the production and surface properties of bamboo-based oxidized biochar; (2) to evaluate the removal of Cd(II) and Cr(VI) under different conditions; (3) to explore the possibility of Cd(II) and Cr(VI) simultaneous adsorption; (4) to study the interaction between Cd(II) and Cr(VI) during adsorption; (5) to demonstrate the adsorption mechanism of the prepared biochar for removal of Cd(II) and Cr(VI) in water.

2. Materials and methods

2.1. Preparation of oxidized biochars

The feedstock for the production of biochar was willow residues pruned from moso bamboo. Moso bamboo obtained in Aichi prefecture, Japan, was cut into chips (8 mm × 10 mm × 5 mm, W × L × T) and was used as a precursor for preparation of the adsorbent.

The bamboo chips were dried in an oven at 110°C for 1 h. In this study, using the $ZnCl_2$ as an activator, the prepared bamboo chips were impregnated with $ZnCl_2$ solution at a ratio of 3 g-$ZnCl_2$/g-bamboo, and then the mixture was dried in an oven at 110°C overnight. The resulting mixture was pyrolyzed for 1 h at 500°C under N_2 atmosphere in a tubular furnace. The prepared biochar was placed in 1 M HCl solution and stirred for 1 h, rinsed in a Soxhlet extractor for 24 h, and dried overnight at 110°C. The obtained samples were referred to as BZ.

The prepared biochars were oxidized in order to load the oxygen-containing functional groups. Using $(NH_4)_2S_2O_8$ solution as an oxidant, BZ (1.0 g) was added into 0.6 kg/L $(NH_4)_2S_2O_8$ solution (50 mL) in a flask, and placed in 30°C water for continuously stirring for 6–48 h. After that, the resulting samples were filtered and washed with hot deionized water for several times until the filtrate pH became neutral, followed by drying in an oven at 110°C overnight. The obtained samples were referred to as BZ-APS*x*h, where *x* is the number of hours for oxidation.

2.2. Characterization

The specific surface area (S_{BET}), mesopore volume (V_{meso}) and micropore volume (V_{micro}) of the prepared biochar were calculated based on N_2 adsorption/desorption isotherms at −196°C using Belsorp-mini II (MicrotracBEL, Co. Ltd., Japan) surface area analyzer. The surface morphology of the biochar was observed by Hitachi S-4800 SEM (Hitachi, Japan). The elemental composition of C, H and N of the adsorbents was determined with PerkinElmer 2400 II (PerkinElmer Japan, Co. Ltd., Japan), and O content was obtained by difference. X-ray photoelectron spectroscopy (XPS) analysis was performed using an ULVAC-PHI Model-1800 spectrometer. FTIR spectrophotometer (IRAffinity-1, SHIMADZU, Japan) was used to analyze surface functional groups of adsorbents. The concentrations of Cr(VI) solution and Cd(II) solution after batch experiments were determined with atomic adsorption spectrometer novAA300 (Analytik Jena AG, Germany).

2.3. Batch adsorption

Batch Cr(VI) adsorption experiments were conducted to examine the adsorption and reduction performance of the prepared biochar as adsorbents. Potassium dichromate ($K_2Cr_2O_7$) and cadmium nitrate ($Cd(NO_3)_2$) were used for preparing the stock solution of Cr(VI) and Cd(II). All batch experiments were carried out in Erlenmeyer flasks. A 0.02 g of the BZ-APS was put into a flask containing 20 mL of solution (Cr(VI) and/or Cd(II)) with various initial concentrations. The flasks were agitated in a water bath shaker at 25°C by the speed of 100 rpm. Sampling and filtration were carried out after a certain contact time. The adsorbed amount of Cr(VI) and Cd(II) on biochar at the equilibrium was calculated by the following equation:

$$Q_e = \left(C_0 - C_e\right)\frac{V}{m} \quad (1)$$

where m (g) is the mass of the biochar, V (L) is the volume of the Cr(VI) and Cd(II) solution, C_0 (mmol/L) represents the initial concentration of Cr(VI) and Cd(II), C_e (mmol/L) is the adsorption equilibrium concentration of Cr(VI) and Cd(II).

The effect of oxidation time of the oxidized biochar on the removal of Cr(VI) and Cd(II) was determined by using BZ-APS6h, BZ-APS12h, BZ-APS24h and BZ-APS48h at concentrations of 1 g/L in a mixed solution of Cr(VI) and Cd(II) under natural pH condition (pH 6). The concentrations of Cr(VI) and Cd(II) in solution were 4 mmol/L each.

The effect of solution pH on Cr(VI) and Cd(II) adsorption was examined by mixing 20 mg of adsorbent with 20 mL of 1.5 mmol/L Cr(VI) and Cd(II) solution. The mixed solution had different pH values, ranging from 2 to 7. The initial pH of phosphate solution was adjusted by 0.1 M HCl and 0.1 M NaOH.

To study the adsorption isotherms, 20 mg of the BZ-APS24h was mixed with 20 mL of either Cr(VI) (0.1–7.7 mmol/L) or Cd(II) (0.1–2.2 mmol/L) at natural pH (pH 6), and then shaken at 100 rpm for 24 h at 25°C, 35°C and 45°C. Finally, the adsorption isotherms for Cr(VI) and Cd(II) were fitted to two isotherm models as follows.

The Langmuir isothermal adsorption model is a theoretical model assuming that the adsorbents were adsorbed in monolayer on the uniform surface of the adsorbent. The linear form of Langmuir equation can be given as follows:

$$\frac{C_e}{Q_e} = \frac{1}{X_m K_L} + \frac{1}{X_m} C_e \tag{2}$$

where Q_e (mmol/g) is the adsorbed amount of Cr(VI) and Cd(II) at equilibrium, C_e (mmol/L) is the equilibrium concentration of Cr(VI) and Cd(II) in the solution, X_m (mmol/g) is the monolayer maximum adsorption capacity, and K_L (L/mmol) is the Langmuir constant related to adsorption energy.

The linear form of Freundlich equation is:

$$\ln Q_e = \ln K_F + \frac{1}{n} \ln C_e \tag{3}$$

where K_F is the Freundlich constant and $1/n$ is the heterogeneity factor. The greater the value of n is, the better the adsorption performance will be.

To study the kinetics of the adsorption process, 0.1 g of the BZ-APS24h was mixed with 20 mL of 4 mmol/L Cr(VI) solution and 4 mmol/L Cd(II) solution under natural pH (pH 6), followed by shaking at 100 rpm.

In the interaction experiment of Cd(II) and Cr(VI), adsorption experiments were carried out by adding BZ-APS24h to a Cr(VI) solution containing a Cd(II) solution with concentration of 0–400 mg/L and a Cd(II) solution containing a Cr(VI) solution with concentration of 0–400 mg/L. The initial pH of all solutions was 6.

3. Results and discussion

3.1. Physicochemical characteristics of biochars

The elemental composition of oxidized biochar with different oxidation time is shown in Table 1. It can be seen from the table that the oxygen content of the non-oxidized BZ is 7.9%. After 6–48 h of oxidation, the content of oxygen in biochar increases proportionally from 22.4% up to 30.1%. This indicates that oxygen functional groups would be loaded with the increase of oxidation time, on the biochar.

Table 1
Elemental composition of each prepared biochar

	C (%)	H (%)	N (%)	O[a] (%)
BZ	90.4	1.5	0.2	7.9
BZ-APS6h	76.2	1.2	0.2	22.4
BZ-APS12h	75.0	1.2	0.2	23.6
BZ-APS24h	72.9	1.3	0.2	25.6
BZ-APS48h	68.3	1.4	0.2	30.1

[a]Calculated by difference.

The morphologies of the BZ and the BZ-APS24h prepared are shown in Fig. 1. It could be seen that nearly no porous structure was observed from a smooth surface of the BZ. The surface of the BZ-APS24h had a relatively fluffy porous structure, which was rougher than that of the BZ. This may be attributed to the destruction of the surface structure of oxidized biochar.

The nitrogen adsorption–desorption isotherm curve of the BZ-APS24h is shown in Fig. 2, and a type I isotherm was observed, which indicates the mainly microporous structure existence. The specific surface area (BET) and micro-/mesoporous structure of the biochar are shown in Table 2. It can be seen that the surface of the biochar before and after oxidation differed greatly. With the increase of oxidation time, the specific surface area of oxidized biochar decreased from 1,726 to 928 m^2/g, and total pore volume decreased from 1.61 to 0.47 cm^3/g. This principally is due to the fact that with increase of oxidation time, more oxygen-containing functional groups were loaded to the surface of biochar. But the plugging pore structure by increase of these functional groups is conducive to the removal of Cd(II).

The functional groups on oxidized biochar were analyzed by XPS. As shown in Fig. S1, the survey spectrums of BZ and BZ-APS24h present two peaks, C1s and O1s energy levels, respectively. Detailed XPS survey of the regions for C1s of BZ and BZ-APS24h is shown in Fig. 3. For the C1s XPS spectrum of the BZ, a strong peak appeared at 285.4 eV, which is attributed to C–C (77%), and the other peaks located at 286.7 and 288.4 eV are assigned to the C–O (13%) and C=O (6%), respectively. After oxidation, the C–O (21%) and C=O (12%) peaks of the BZ-APS24h contain obvious increment compared with BZ. This indicates that the functional groups on the surface of oxidized biochar are mostly –COOH, with a small amount of -OH.

3.2. Effect of initial oxidation time

From Tables 1 and 2, it can be known that the increase of oxidation time caused the increase of surface functional groups on the oxidized biochar, so their adsorption capacity for Cr(VI) and Cd(II) should be different. Fig. 4 shows the adsorption capacity of Cr(VI) and Cd(II) with different oxidation time. It was observed that when oxidation time increased from 6 to 24 h, the adsorption capacity of Cr(VI)

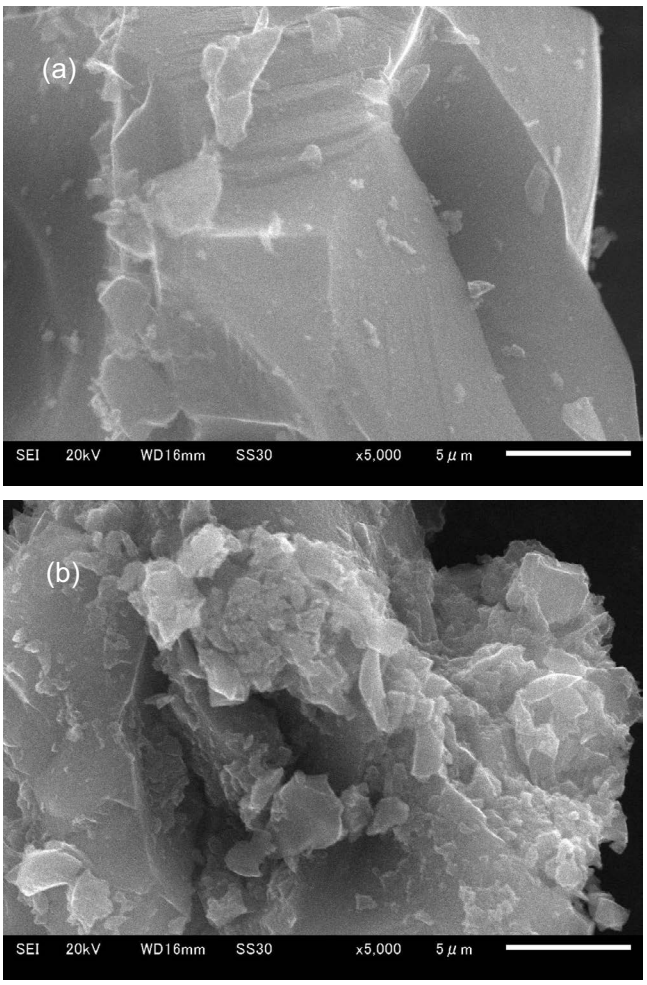

Fig. 1. SEM images of BZ (a) and BZ-APS24h (b).

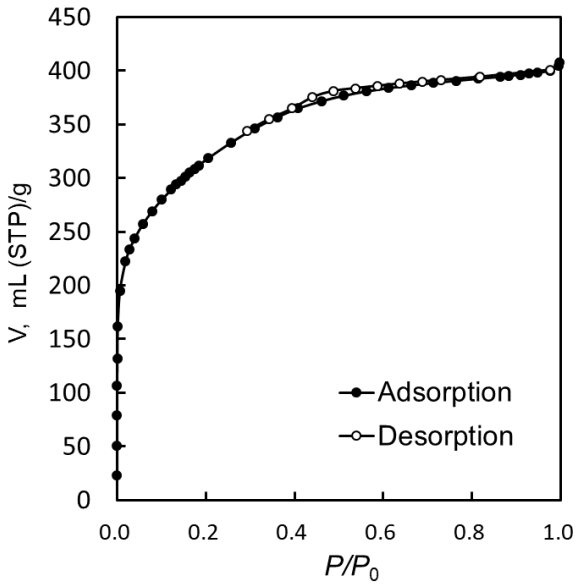

Fig. 2. Nitrogen adsorption isotherm of BZ-APS24h.

and Cd(II) increased; when the oxidation time increased from 24 to 48 h, the adsorbed amount of Cd(II) remained unchanged, but the adsorbed amount of Cr(VI) decreased. Meanwhile, the equilibrium pH of the solution decreased with the increase of oxidation time of biochar. The existence of chromium in the solution after adsorption was measured as shown in Fig. 4a. This shows that the adsorption performance of oxidized biochar for mixed solution of Cr(VI) and Cd(II) reached the highest point when the oxidation time was 24 h. At the same time, the existence of chromium in the solution after adsorption was measured as shown in Fig. 4b. It can be inferred that the remaining chromium in the solution was mainly Cr(VI), and no Cr(VI) was reduced to Cr(III) under these conditions.

3.3. Effect of solution pH

Initial solution pH has a significant impact on the removal efficiency of Cr(VI) and Cd(II) in aqueous solution. Cadmium species are found to be present in deionized water in the forms of Cd^{2+}, $Cd(OH)^{+}$, $Cd(OH)_2^0$, $Cd(OH)_2$(s), etc [34]. Cd^{2+} begins to precipitate when pH > 7, thus, the effect of pH was studied within the range from 2 to 7. The effects of solution pH on Cr(VI) adsorption, Cd(II) adsorption and co-adsorption of Cr(VI) and Cd(II) with oxidized biochar BZ-APS24h samples were investigated as shown in Fig. 5.

For adsorption of Cr(VI), the adsorbed amount of Cr(VI) on BZ-APS24 decreased as pH increased from 2 to 7. This is because the solution pH value significantly affected the structure of the adsorbents, the surface charges of the adsorbent and the surface-reactive functional groups in the solution. Cr(VI) exists in different ionic forms in aqueous solution. When solution pH is greater than 6, it presents as CrO_4^{2-}; when pH is ranging from 1.0 to 6.0, it exists as $Cr_2O_7^{2-}$ and $HCrO_4^-$ [35], which are favorably adsorbed by BZ-APS24h at low pH because of the electrostatic attraction. When the initial pH was from 2 to 6, equilibrium solution

Table 2
Textural and surface properties of each prepared biochar

Sample	S_{BET} (m^2/g)	V_{total} (cm^3/g)	V_{micro} (cm^3/g)	V_{meso} (cm^3/g)
BZ	1,726	1.61	1.55	0.06
BZ-APS6h	1,484	1.06	1.02	0.04
BZ-APS12h	1,352	0.95	0.93	0.02
BZ-APS24h	1,120	0.62	0.61	0.01
BZ-APS48h	928	0.47	0.45	0.02

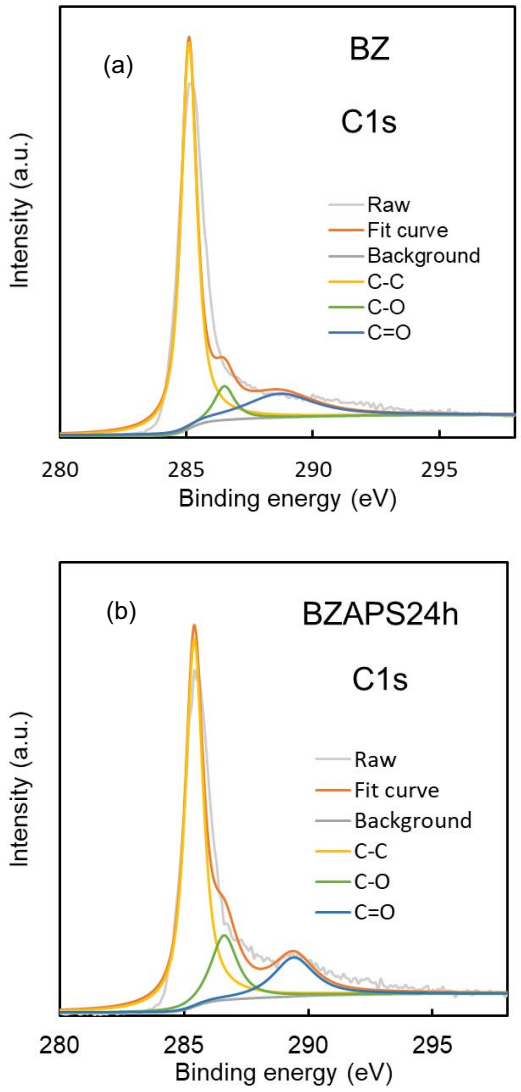

Fig. 3. XPS survey spectra of BZ (a) and BZ-APS24h (b).

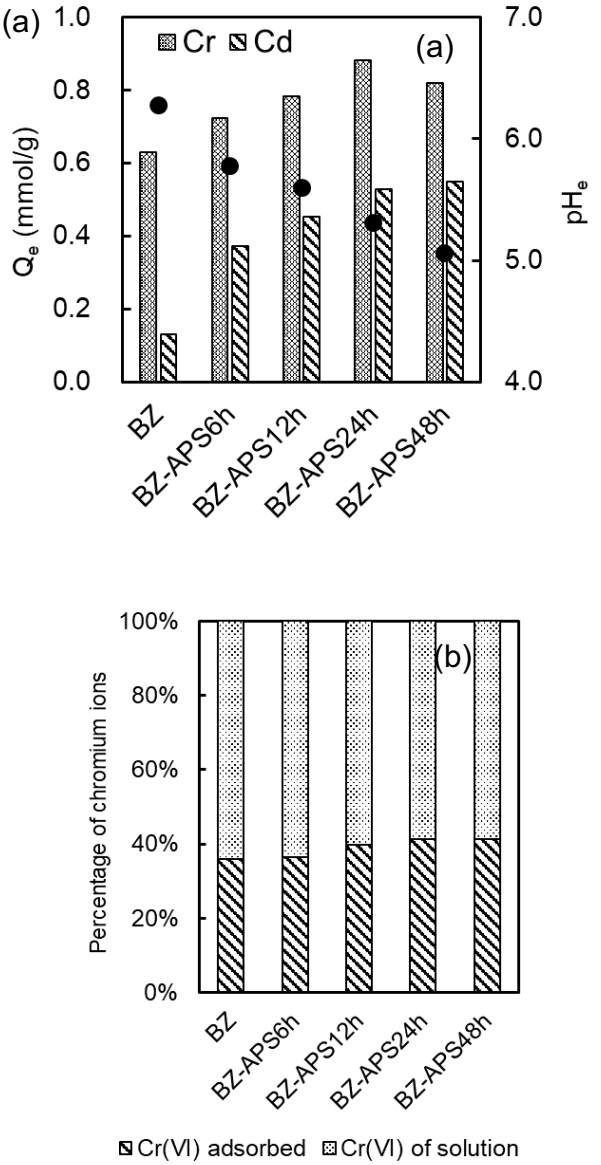

Fig. 4. (a) Simultaneous removal of Cd(II) and Cr(VI) by different materials and (b) the forms of chromium after adsorption.

pH was found to increase. Increase in pH can be explained by solute–sorbent binding reactions. When the oxo groups on the surface of the biochar are in contact with the solution, the following reaction occurs [36]:

$$C_xO + HCrO_4^- + 2H_2O \rightarrow C_xO_2H_3CrO_3^+ + 2OH^- \quad (4)$$

$$CrO_4^{2-} + 2H^+ \rightarrow Cr_2O_7^{2-} + H_2O \quad (5)$$

On the contrary, for adsorption of Cd(II) alone, the adsorbed amount increased as the pH increased from 2 to 5. When the initial pH was changed from 5 to 7, the equilibrium pH of the solution dropped to 3.5–4, while the adsorption amount did not significantly change. In the adsorption process of Cd(II) on biochar, Cd(II) ions were exchanged with protons on the surface carboxy group or other functional groups of the oxidized biochar, causing the decrease in the solution pH; when the pH of the solution dropped to a certain level, the ion exchange was no longer progressed. Through the adjustment of the equilibrium pH of the solution by adding NaOH to the solution, the effect of equilibrium pH on the adsorption amount of Cd(II) was obtained, as shown in Fig. 5c. It can also be seen from Fig. 5c that the equilibrium pH had a greater effect on Cd(II) adsorption than initial pH. As the equilibrium pH increased, the adsorbed amount of Cd(II) increased. The higher pH may lead to the transformation of –COOH groups present in the biochar into $–COO^-$, which was conductive to the adsorption of Cd^{2+}.

Fig. 5d shows the effect of initial pH in mixed solution of Cr(VI) and Cd(II). It could be clearly seen that the co-adsorption of Cd(II) and Cr(VI) was the same as adsorption of the Cr(VI) or Cd(II), and the pH change before and after adsorption was not significant. With the increase of the initial pH, the adsorbed amount of Cd(II) in the mixed solution

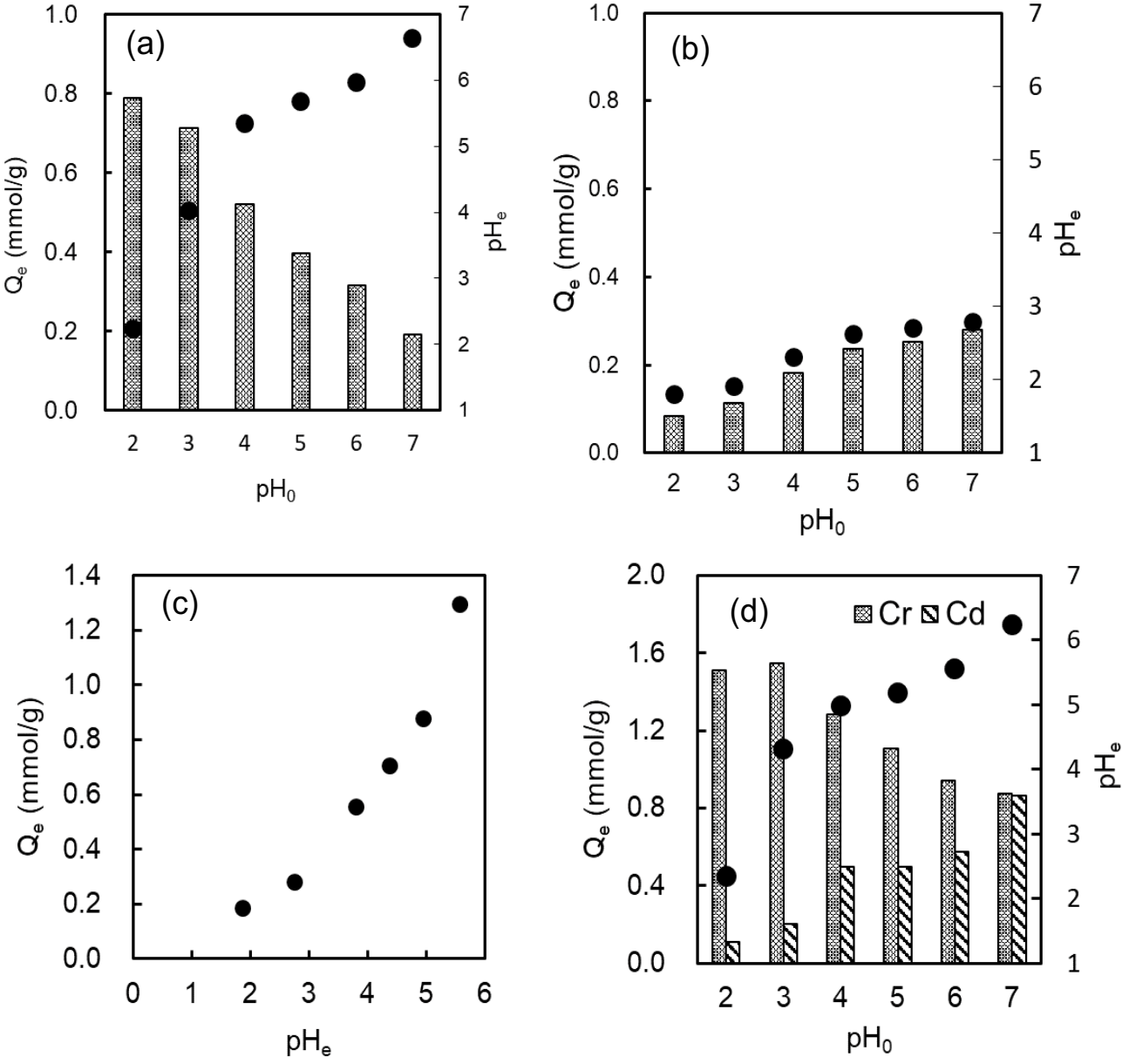

Fig. 5. (a) Effect of initial pH value on Cr(VI) removal, (b) effect of initial pH value on Cd(II) removal, (c) effect of equilibrium pH value on Cd(II) removal and (d) effect of initial pH value on Cd(II) and Cr(VI) simultaneous removal.

gradually increased, while the adsorbed amount of Cr(VI) gradually decreased. Usually, the pH in natural water is about 6. Therefore, the initial pH value of 6 was selected for the further studies on Cr(VI) and Cd(II) ions adsorption.

3.4. Effect of contact time and adsorption kinetics

The contact time between the adsorbate and the adsorbent is an important factor affecting the water treatment. It can be seen from Fig. 5 that the pH of the solution changes with the adsorption, so it is important to study the change of pH with time during the adsorption process. Fig. 6 shows the time course of removal efficiency of Cr(VI) and Cd(II) together with the change of pH. It can be seen that both the Cd(II) and Cr(VI) adsorption equilibriums can be reached within 180 min in Cd(II) solution, Cr(VI) solution and mixed solution of Cd(II) and Cr(VI) mixed solution. As shown in Figs. 6a1 and a2, for the removal of Cd(II) alone, the pH of the solution dropped from 6.1 to 3.3 since the start of adsorption is due to the exchange of Cd^{2+} and H^+ ions during adsorption. When the adsorption reached equilibrium, the pH of the solution tended to be stable at 3.3. In contrast, it can be seen from Figs. 6b1 and b2 that for the removal of Cr(VI) alone, the pH of the solution first decreased from 6.1 to 5.5 and then gradually increased to 5.7, which was a less significant change compared with the adsorption of Cd(II) alone. In the mixed solution of Cd(II) and Cr(VI), Fig. 6c1 indicates that both Cr(VI) and Cd(II) were well adsorbed,

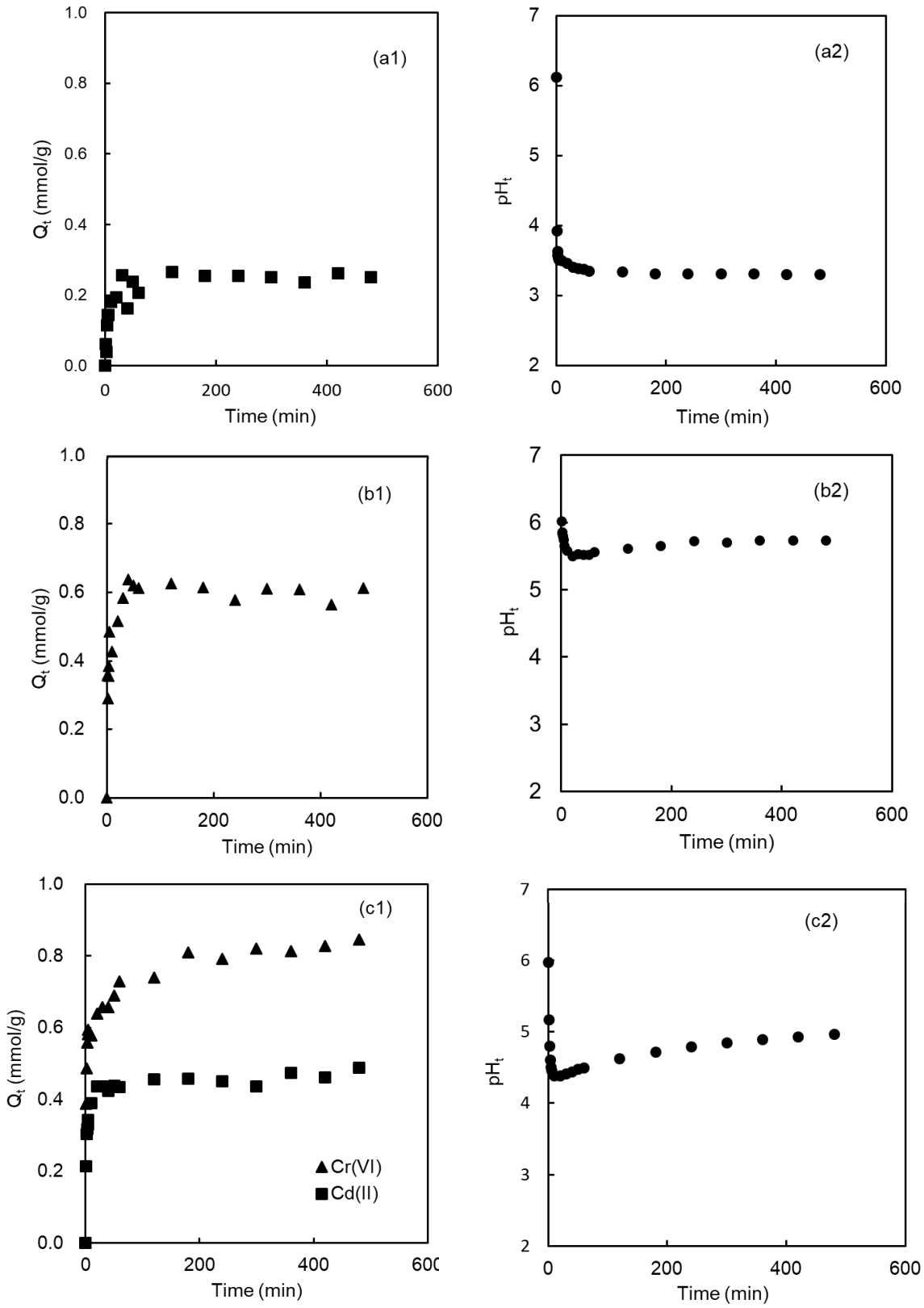

Fig. 6. Effect of contact time: (a1) changes in adsorption quantities in Single Cd(II) removal, (a2) changes in solution pH for single Cd(II) removal, (b1) changes in adsorption quantities for single Cr(VI) removal, (b2) changes in solution pH for single Cr(VI) removal, (c1) changes in adsorption quantities for Cd(II) and Cr(VI) simultaneous removal, and (c2) changes in solution pH for Cd(II) and Cr(VI) simultaneous removal.

and Fig. 6c2 indicates that the pH of the solution dropped rapidly from 6.1 to 4.4 within 20 min, then gradually rose to 5.0 from 20 to 480 min. This is mainly due to that the adsorption of cadmium first led to a decrease in pH, and then the adsorption of chromium caused the rise of pH.

To test the adsorption kinetics in this experiment, the pseudo-first-order kinetic and pseudo-second-order kinetic are expressed as Eqs. (6) and (7),

$$\ln\left(Q_e - Q_t\right) = \ln Q_e - k_1 t \tag{6}$$

$$\frac{t}{Q_t} = \frac{1}{k_2 Q_e^2} + \frac{t}{Q_e} \tag{7}$$

where Q_e is the adsorbed amount of Cd(II) and Cr(VI) at equilibrium (mmol/g), Q_t is the adsorbed amount of Cd(II) and Cr(VI) (mmol/g) at time t (min). k_1 is the rate constant of the pseudo-first-order model (1/min), k_2 is the rate constant of the pseudo-second-order model (g/mmol min). The results of the kinetic analysis are shown in Tables 3 and 4.

The pseudo-first-order model has lower correlation coefficient (R^2) compared with that of the pseudo-second-order models, and all R^2 values are greater than 0.99 for pseudo-second-order models. This indicates that the pseudo-second-order kinetic model is more appropriate than pseudo-first-order kinetic model in describing the adsorption process of Cd(II) and Cr(VI) onto BZ-APS24h. These facts suggest that the adsorption behavior is mainly governed by diffusion control mechanism in Cd(II) solution, Cr(VI) solution and mixed solution of Cd(II) and Cr(VI) [37,38].

3.5. Equilibrium adsorption isotherms

The adsorption isotherms of individual Cr(VI) and Cd(II) on BZ-APS24h are shown in Fig. 7. Langmuir and Freundlich models were applied to investigate the adsorption process of Cr(VI) and Cd(II) at 25°C, 35°C and 45°C. The different isotherm constants determined are shown in Tables 5 and 6. The Langmuir model was more fitted than the Freundlich model, with R^2 ranging from 0.989 to 0.998 for the BZ-APS24h. The Langmuir isotherm is usually used to describe the mono-layer adsorption on a homogenous surface. Therefore, the adsorption of Cr(VI) and Cd(II) on the BZ-APS24h should be monolayer, showing uniform surface properties [39].

By comparing the maximum adsorption capacity (X_m) at different temperatures, it can be seen that the adsorption amount of Cd(II) decreased with the increase of temperature, and the maximum adsorption amount of Cr(VI) increased with the increase of temperature. This indicates that the adsorption of Cr(VI) by oxidized biochar is an endothermic reaction, while the adsorption of Cd(II) is an exothermic reaction. This result is consistent with the previous reports [40,41].

3.6. Mutual influence of Cd(II) and Cr(VI)

Fig. 8a shows the results of adsorption experiments for Cr(VI) solution containing different concentrations of Cd(II). As the Cd(II) concentration in the solution increased from 0 to 400 mg/L, the adsorbed amount of Cr(VI) increased from 0.62 to 0.97 mmol/g, and the equilibrium pH dropped from 5.5 to 4.1. This may be due to that the adsorption of Cd(II) led to a decreased solution pH that was favorable for the adsorption of Cr(VI), so the presence of Cd(II) is beneficial to the adsorption of Cr(VI) on oxidized biochar. Similarly, the solution pH rose due to the adsorption and reduction of Cr(VI), as the Cd(II) concentration in the solution increased from 0 to 400 mg/L, the equilibrium pH went up from 3.0 to 5.3, and the adsorbed amount of Cr(VI) increased from 0.28 to 0.79 mmol/g, as shown in Fig. 8b. This indicates that the presence of Cr(VI) is contributed to the adsorption of and Cd(II), this is because the adsorption of Cr(VI) results in the increase of solution pH, and the increase of pH is favorable for the adsorption of Cd(II).

3.7. Possible adsorption mechanism

The oxygen functional groups of biochar play a vital role in the adsorption process. The adsorption of Cd(II) onto

Table 3
Kinetic parameters for single Cd(II) and Cr(VI) adsorption

	Pseudo-first-order			Pseudo-second-order		
	Q_e	k_1		Q_e	k_2	
	(mmol/g)	(min^{-1})	R^2	(mmol/g)	(g/mmol min)	R^2
Cd(II)	1.34	0.07	0.766	0.26	0.67	0.996
Cr(VI)	1.78	0.06	0.812	0.60	3.25	0.997

Table 4
Kinetic parameters for simultaneous Cd(II) and Cr(VI) adsorption

	Pseudo-first-order			Pseudo-second-order		
	Q_e (mmol/g)	k_1 (min^{-1})	R^2	Q_e (mmol/g)	k_2 (g/mmol min)	R^2
Cd(II)	1.42	0.24	0.964	0.47	0.52	0.999
Cr(VI)	2.76	0.14	0.721	0.84	0.19	0.999

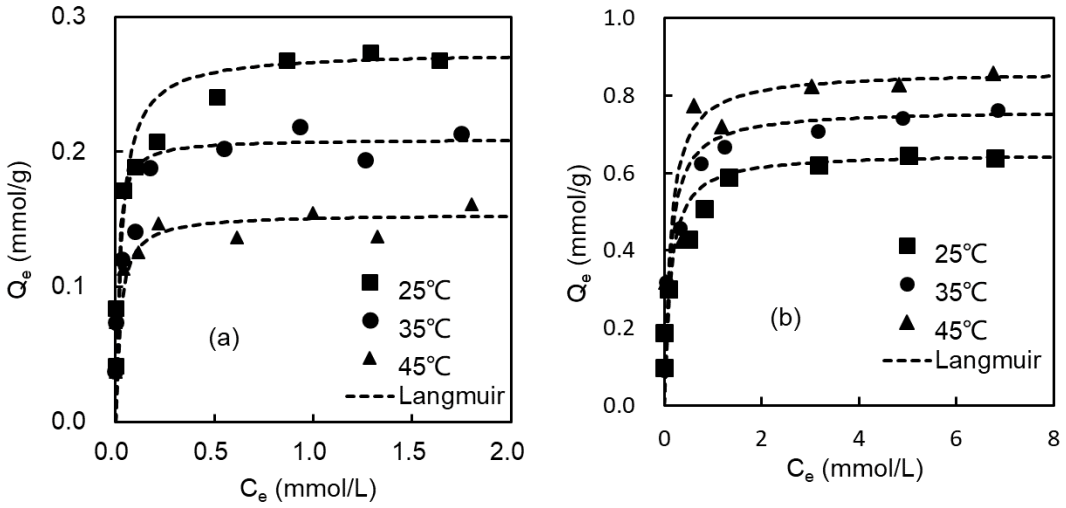

Fig. 7. Adsorption isotherms of Cd(II) (a) and Cr(VI) (b) onto BZ-APS24h.

Table 5
Langmuir and Freundlich adsorption isotherm parameters of Cd(II) in aqueous solutions

	Langmuir model			Freundlich model		
Temperature	X_m (mmol/g)	K_1 (L/mmol)	R^2	K_f([mmol/g][mmol/L])^n	1/n	R^2
25°C	0.27	33.9	0.998	0.022	0.27	0.787
35°C	0.21	28.5	0.996	0.027	0.16	0.944
45°C	0.15	25.6	0.989	0.012	0.09	0.916

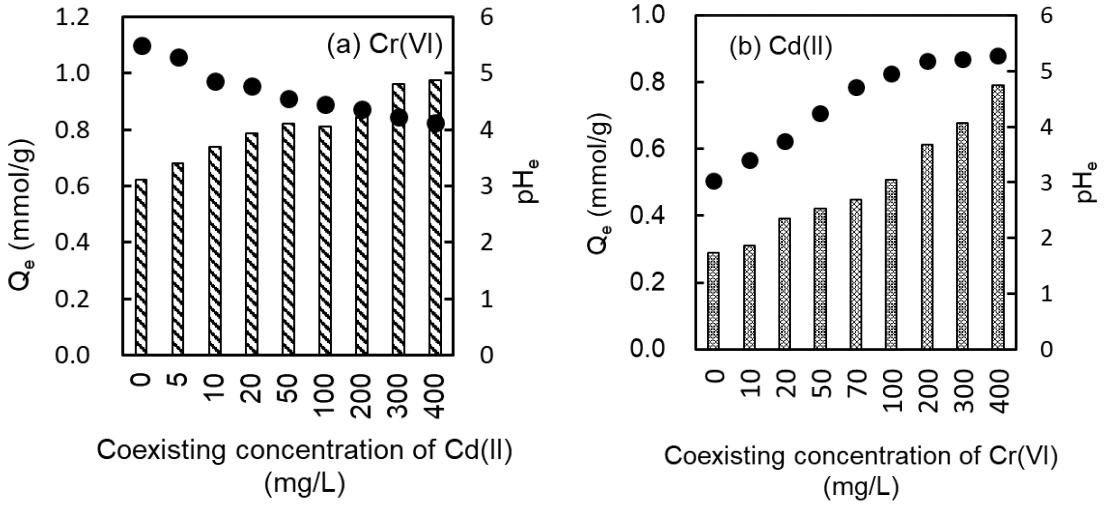

Fig. 8. Mutual influence of coexisting Cd(II) and Cr(VI): adsorption of Cr(VI) (a) and Cd(II) (b).

the BZ-APS24h mainly depends on the oxygen functional groups. As shown in Fig. 9, the FTIR analysis reveals the surface functional groups of prepared biochar. The peak located at about 1,612 and 3,564 cm might assign O=C–O and –OH [42], respectively. It can be seen that the peak of –COOH on BZ-APS24h was larger than that on BZ. After the simultaneous adsorption of Cd(II) and Cr(VI), the peaks at –COOH and –OH of BZ-APS24h became larger. This is due to the strong oxidability of Cr(VI), and the surface of biochar was oxidized in the process of adsorption.

In order to determine the adsorption mechanism, XPS analysis of BZ-APS24h after Cr(VI) and Cd(II) adsorption was performed. As shown in Fig. 10a, the Cd3d5 spectrum was divided into only one peak in 406 eV, which indicates

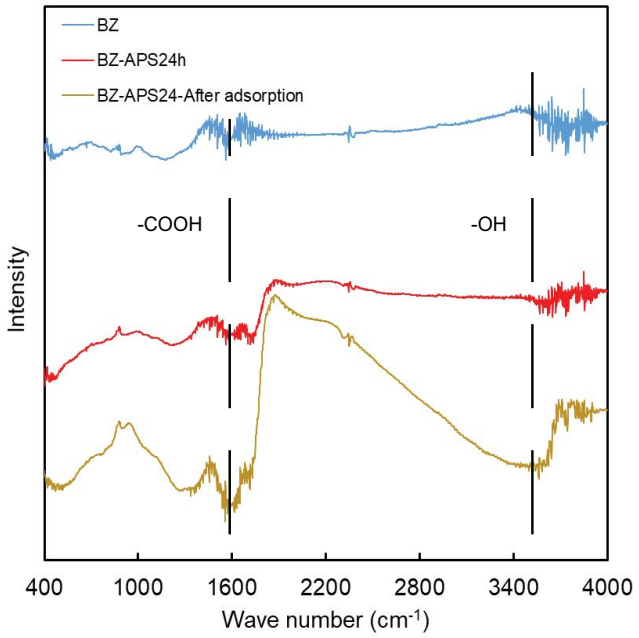

Fig. 9. FTIR spectra of BZ, BZ-APS24h and BZ-APS24h after adsorption.

that Cd(II) was adsorbed on the surface of biochar by Cd^{2+} ions. As shown in Fig. 10b, for the removal of Cr(VI), two peaks appeared at 577.8 and 580.4 eV in the Cr2p3/2 region, which might be due to Cr(VI) and Cr(III), respectively [43]. It was found that most of Cr existed in the form of Cr(III) rather than Cr(VI) on the BZ-APS24h surface. The existence of Cr(III) is originated from the reduction of Cr(VI) by the π electrons of the carbocyclic six-membered ring [44]. Based on the analysis in Fig. 6, it can be concluded that the adsorption rate of Cd(II) was faster, so Cd^{2+} was first exchanged with H^+ of the –COOH on the surface of the BZ-APS24h, resulting in a drop in the pH of the solution. At the same time, due to the drop in pH of the solution, which became conducive to the adsorption of Cr(VI). The adsorption of Cr(VI) was also carried out simultaneously. A portion of Cr(VI) was directly adsorbed on the surface of biochar, and another portion of Cr(VI) was reduced to Cr(III). OH^- ions are released during the reduction and adsorption of Cr(VI), and the H^+ ions released during Cd(II) adsorption are neutralized.

4. Conclusion

In summary, oxidized biochar (BZ-APS24h) was successfully prepared using bamboo. The prepared BZ-APS24h is rich in oxygen-containing functional groups and reserves a

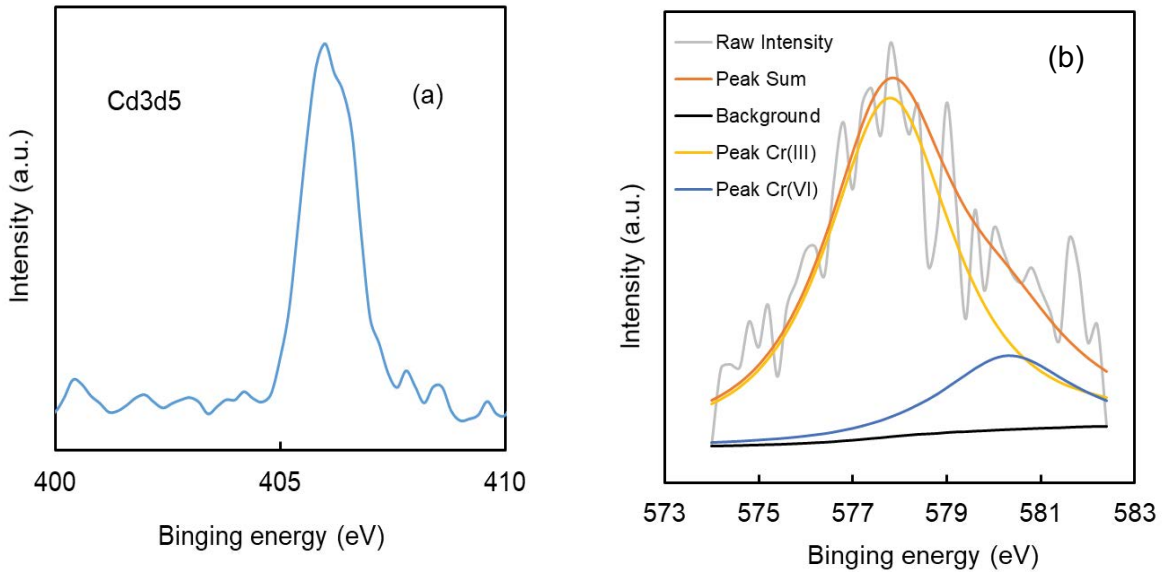

Fig. 10. XPS survey spectra of Cd3d5 (a) and Cr2p3/2 (b) for the BZ-APS24h after adsorption.

Table 6
Langmuir and Freundlich adsorption isotherm parameters of Cr(VI) in aqueous solutions

	Langmuir model			Freundlich model		
Temperature	X_m (mmol/g)	K_1 (L/mmol)	R^2	K_f([mmol/g][mmol/L])^n	1/n	R^2
25°C	0.65	8.36	0.998	0.20	0.17	0.976
35°C	0.76	9.43	0.998	0.28	0.19	0.972
45°C	0.86	11.19	0.997	0.35	0.21	0.934

high specific surface area. The BZ-APS24h exhibited excellent adsorption performance for the removal Cd(II) and Cr(VI), with adsorption capacity of 0.65 mmol/g (33.8 mg/g) for removal of Cr(VI) removal, and 0.27 mmol/g (30.3 mg/g) for removal of Cd(II) at 25°C. BZ-APS24h is capable of simultaneously adsorbing Cd(II) and Cr(VI) in a mixed solution of Cd(II) and Cr(VI). The pH of the solution has a great influence on the adsorption process. Cd(II) adsorption causes a decrease in pH, while adsorption of Cr(VI) causes an increase in pH. Acidic pH is favorable for the adsorption of Cr(VI), while neutral pH is favorable for the adsorption of Cd(II). The coexistence of Cd(II) and Cr(VI) can promote the adsorption of the other ion. Thus, BZ-APS24h is demonstrated to be an excellent adsorbent for simultaneous removal of Cd(II) and Cu(VI) from aqueous solution.

Acknowledgments

Gratitude is greatly extended by the authors to Prof. Dr. Fumio Imazeki, the head of Safety and Health Organization, Chiba University, for his financial support on the study. The authors are also thankful to Cosmo Oil Co., Ltd., for XPS analysis. Bei Chu also acknowledges the kind support of the Japanese Government (MEXT) for the scholarship.

References

[1] K. Selvi, S. Pattabhi, K. Kadirvelu, Removal of Cr(VI) from aqueous solution by adsorption onto activated carbon, Bioresour. Technol., 80 (2001) 87–89.
[2] F.Y. Wang, H. Wang, J.W. Ma, Adsorption of cadmium (II) ions from aqueous solution by a new low-cost adsorbent—bamboo charcoal, J. Hazard. Mater., 177 (2010) 300–306.
[3] Y.S. Ok, A.R. Usman, S.S. Lee, S.A.A. El-Azeem, B. Choi, Y. Hashimoto, J.E. Yang, Effects of rapeseed residue on lead and cadmium availability and uptake by rice plants in heavy metal contaminated paddy soil, Chemosphere, 85 (2011) 677–682.
[4] W. Qi, Y. Zhao, X. Zheng, M. Ji, Z. Zhang, Adsorption behavior and mechanism of Cr (VI) using Sakura waste from aqueous solution, Appl. Surf. Sci., 360 (2016) 470–476.
[5] X. Lv, J. Xu, G. Jiang, X. Xu, Removal of chromium (VI) from wastewater by nanoscale zero-valent iron particles supported on multiwalled carbon nanotubes, Chemosphere, 85 (2011) 1204–1209.
[6] H. Shen, Y.-T. Wang, Simultaneous chromium reduction and phenol degradation in a coculture of *Escherichia coli* ATCC 33456 and *Pseudomonas putida* DMP-1, Appl. Environ. Microbiol., 61 (1995) 2754–2758.
[7] X. Yi, F. Xiao, X. Zhong, Y. Duan, K. Liu, C. Zhong, A Ca^{2+} chelator ameliorates chromium (VI)-induced hepatocyte L-02 injury via down-regulation of voltage-dependent anion channel 1 (VDAC1) expression, Environ. Toxicol. Pharmacol., 49 (2017) 27–33.
[8] Q. Chen, J. Zheng, L. Zheng, Z. Dang, L. Zhang, Classical theory and electron-scale view of exceptional Cd (II) adsorption onto mesoporous cellulose biochar via experimental analysis coupled with DFT calculations, Chem. Eng. J., 350 (2018) 1000–1009.
[9] X. Zhang, L. Lv, Y. Qin, M. Xu, X. Jia, Z. Chen, Removal of aqueous Cr (VI) by a magnetic biochar derived from Melia azedarach wood, Bioresour. Technol., 256 (2018) 1–10.
[10] S.J. Ye, G.M. Zeng, H.P. Wu, C. Zhang, J. Liang, J. Dai, Z.F. Liu, W.P. Xiong, J. Wan, P.A. Xu, M. Cheng, Co-occurrence and interactions of pollutants, and their impacts on soil remediation-A review, Crit. Rev. Environ. Sci. Technol., 47 (2017) 1528–1553.
[11] A.A. Nezhad, M. Alimoradi, M. Ramezani, Highly efficient removal of Cd (II) ions by composite of GO and layered double hydroxide composite, Mater. Res. Express, 6 (2018) 015015.
[12] Y. Huang, X. Lee, F.C. Macazo, M. Grattieri, R. Cai, S.D. Minteer, Fast and efficient removal of chromium (VI) anionic species by a reusable chitosan-modified multi-walled carbon nanotube composite, Chem. Eng. J., 339 (2018) 259–267.
[13] S.P. Verma, B. Sarkar, Simultaneous removal of Cd (II) and p-cresol from wastewater by micellar-enhanced ultrafiltration using rhamnolipid: flux decline, adsorption kinetics and isotherm studies, J. Environ. Manage., 213 (2018) 217–235.
[14] L. Li, J. Zhang, Y. Li, C. Yang, Removal of Cr (VI) with a spiral wound chitosan nanofiber membrane module via dead-end filtration, J. Membr. Sci., 544 (2017) 333–341.
[15] L. Alvarado, I.R. Torres, A. Chen, Integration of ion exchange and electrodeionization as a new approach for the continuous treatment of hexavalent chromium wastewater, Sep. Purif. Technol., 105 (2013) 55–62.
[16] L. Dong, L.a. Hou, Z. Wang, P. Gu, G. Chen, R. Jiang, A new function of spent activated carbon in BAC process: Removing heavy metals by ion exchange mechanism, J. Hazard. Mater., 359 (2018) 76–84.
[17] R. Xiao, J.J. Wang, R. Li, J. Park, Y. Meng, B. Zhou, S. Pensky, Z. Zhang, Enhanced sorption of hexavalent chromium [Cr (VI)] from aqueous solutions by diluted sulfuric acid-assisted MgO-coated biochar composite, Chemosphere, 208 (2018) 408–416.
[18] L. Shen, Z. Jin, D. Wang, Y. Wang, Y. Lu, Enhance wastewater biological treatment through the bacteria induced graphene oxide hydrogel, Chemosphere, 190 (2018) 201–210.
[19] Y. Zuo, G. Chen, G. Zeng, Z. Li, M. Yan, A. Chen, Z. Guo, Z. Huang, Q. Tan, Transport, fate, and stimulating impact of silver nanoparticles on the removal of Cd (II) by *Phanerochaete chrysosporium* in aqueous solutions, J. Hazard. Mater., 285 (2015) 236–244.
[20] L. Ling, W.-J. Liu, S. Zhang, H. Jiang, Achieving high-efficiency and ultrafast removal of Pb (II) by one-pot incorporation of a N-doped carbon hydrogel into FeMg layered double hydroxides, J. Mater. Chem. A, 4 (2016) 10336–10344.
[21] S. Ye, M. Yan, X. Tan, J. Liang, G. Zeng, H. Wu, B. Song, C. Zhou, Y. Yang, H. Wang, Facile assembled biochar-based nanocomposite with improved graphitization for efficient photocatalytic activity driven by visible light, Appl. Catal., B, 250 (2019) 78–88.
[22] B. Jiang, Y. Lin, J.C. Mbog, Biochar derived from swine manure digestate and applied on the removals of heavy metals and antibiotics, Bioresour. Technol., 270 (2018) 603–611.
[23] S. Ye, G. Zeng, H. Wu, C. Zhang, J. Dai, J. Liang, J. Yu, X. Ren, H. Yi, M. Cheng, Biological technologies for the remediation of co-contaminated soil, Crit. Rev. Biotechnol., 37 (2017) 1062–1076.
[24] S.J. Ye, G.M. Zeng, H.P. Wu, J. Liang, C. Zhang, J. Dai, W.P. Xiong, B. Song, S.H. Wu, J.F. Yu, The effects of activated biochar addition on remediation efficiency of co-composting with contaminated wetland soil, Resour. Conserv. Recycl., 140 (2019) 278–285.
[25] D. Jiang, B. Chu, Y. Amano, M. Machida, Removal and recovery of phosphate from water by Mg-laden biochar: batch and column studies, Colloids Surf., A, 558 (2018) 429–437.
[26] Y. Su, X. Sun, X. Zhou, C. Dai, Y. Zhang, Zero-valent iron doped carbons readily developed from sewage sludge for lead removal from aqueous solution, J. Environ. Sci., 36 (2015) 1–8.
[27] R. Li, L. Zhang, P. Wang, Rational design of nanomaterials for water treatment, Nanoscale, 7 (2015) 17167–17194.
[28] M.F. El-Banna, A. Mosa, B. Gao, X. Yin, Z. Ahmad, H. Wang, Sorption of lead ions onto oxidized bagasse-biochar mitigates Pb-induced oxidative stress on hydroponically grown chicory: experimental observations and mechanisms, Chemosphere, 208 (2018) 887–898.
[29] M. Machida, B. Fotoohi, Y. Amamo, T. Ohba, H. Kanoh, L. Mercier, Cadmium (II) adsorption using functional mesoporous silica and activated carbon, J. Hazard. Mater., 221 (2012) 220–227.
[30] W.J. Yin, Z.Z. Guo, C.C. Zhao, J.T. Xu, Removal of Cr(VI) from aqueous media by biochar derived from mixture biomass precursors of *Acorus calamus* Linn. and feather waste, J. Anal. Appl. Pyrolysis, 140 (2019) 86–92.

[31] Q. Tao, Y.X. Chen, J.W. Zhao, B. Li, Y.H. Li, S.Y. Tao, M. Li, Q.Q. Li, Q. Xu, Y.D. Li, H.X. Li, B. Li, Y.L. Chen, C.Q. Wang, Enhanced Cd removal from aqueous solution by biologically modified biochar derived from digestion residue of corn straw silage, Sci. Total Environ., 674 (2019) 213–222.
[32] D. Wang, G. Zhang, Z. Dai, L. Zhou, P. Bian, K. Zheng, Z. Wu, D. Cai, Sandwich-like nano-system for simultaneous removal of Cr(VI) and Cd(II) from water and soil, ACS Appl. Mater. Interfaces, 10 (2018) 18316–18326.
[33] Z.-H. Diao, J.-J. Du, D. Jiang, L.-J. Kong, W.-Y. Huo, C.-M. Liu, Q.-H. Wu, X.-R. Xu, Insights into the simultaneous removal of Cr^{6+} and Pb^{2+} by a novel sewage sludge-derived biochar immobilized nanoscale zero valent iron: coexistence effect and mechanism, Sci. Total Environ., 642 (2018) 505–515.
[34] V.C. Srivastava, I.D. Mall, I.M. Mishra, Adsorption of toxic metal ions onto activated carbon: study of sorption behaviour through characterization and kinetics, Chem. Eng. Process. Process Intensif., 47 (2008) 1269–1280.
[35] M. Goswami, L. Borah, D. Mahanta, P. Phukan, Equilibrium modeling, kinetic and thermodynamic studies on the adsorption of Cr(VI) using activated carbon derived from matured tea leaves, J. Porous Mater., 21 (2014) 1025–1034.
[36] S. Mor, K. Ravindra, N. Bishnoi, Adsorption of chromium from aqueous solution by activated alumina and activated charcoal, Bioresour. Technol., 98 (2007) 954–957.
[37] Y. Zhou, Q. Jin, T. Zhu, Y. Akama, Adsorption of chromium (VI) from aqueous solutions by cellulose modified with β-CD and quaternary ammonium groups, J. Hazard. Mater., 187 (2011) 303–310.
[38] M. Bhaumik, A. Maity, V. Srinivasu, M.S. Onyango, Enhanced removal of Cr (VI) from aqueous solution using polypyrrole/Fe_3O_4 <<<magnetic nanocomposite, J. Hazard. Mater., 190 (2011) 381–390.
[39] K.Y. Foo, B.H. Hameed, Insights into the modeling of adsorption isotherm systems, Chem. Eng. J., 156 (2010) 2–10.
[40] J. Sun, Z. Zhang, J. Ji, M. Dou, F. Wang, Removal of Cr^{6+} from wastewater via adsorption with high-specific-surface-area nitrogen-doped hierarchical porous carbon derived from silkworm cocoon, Appl. Surf. Sci., 405 (2017) 372–379.
[41] Y. Shi, T. Zhang, H. Ren, A. Kruse, R. Cui, Polyethylene imine modified hydrochar adsorption for chromium (VI) and nickel (II) removal from aqueous solution, Bioresour. Technol., 247 (2018) 370–379.
[42] P.F.R. Ortega, J.P.C. Trigueiro, M.R. Santos, A.M.L. Denadai, L.C.A. Oliveira, A.P.C. Teixeira, G.G. Silva, R.L. Lavall, Thermodynamic study of Methylene Blue adsorption on carbon nanotubes using isothermal titration calorimetry: a simple and rigorous approach, J. Chem. Eng. Data, 62 (2017) 729–737.
[43] D. Park, Y.-S. Yun, J.H. Jo, J.M. Park, Mechanism of hexavalent chromium removal by dead fungal biomass of *Aspergillus niger*, Water Res., 39 (2005) 533–540.
[44] M. Li, Y. Gong, A. Lyu, Y. Liu, H. Zhang, The applications of populus fiber in removal of Cr(VI) from aqueous solution, Appl. Surf. Sci., 383 (2016) 133–141.

Supplementary information

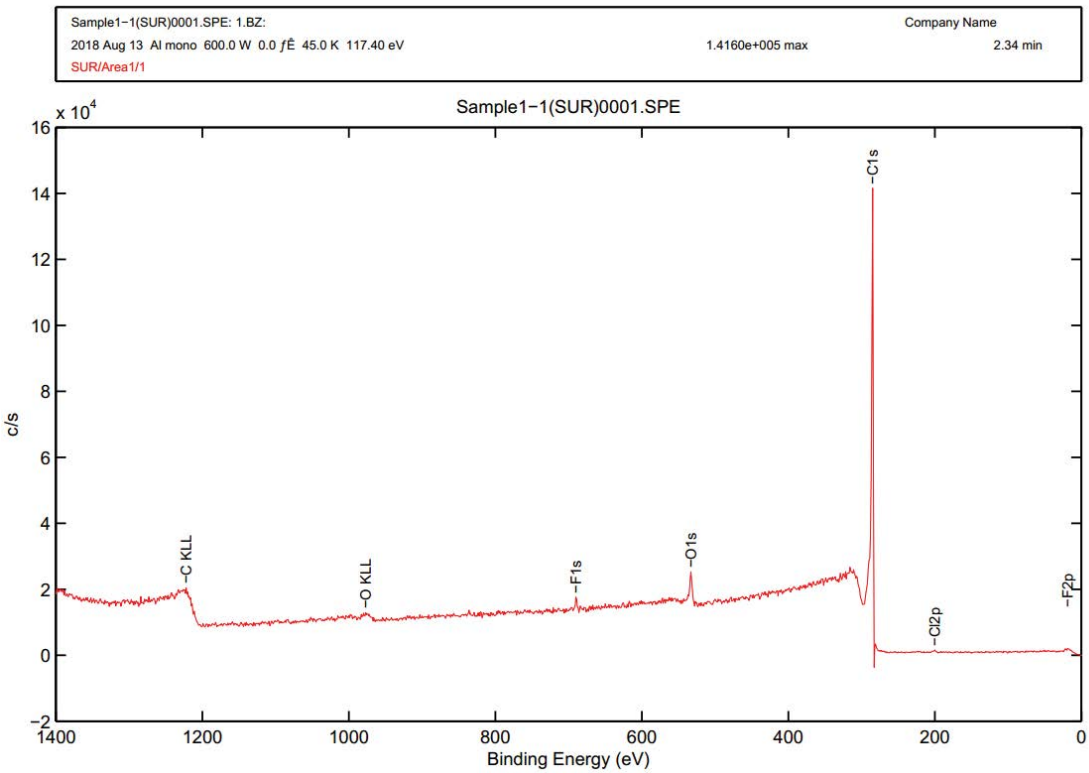

Fig. S1. *Continued*

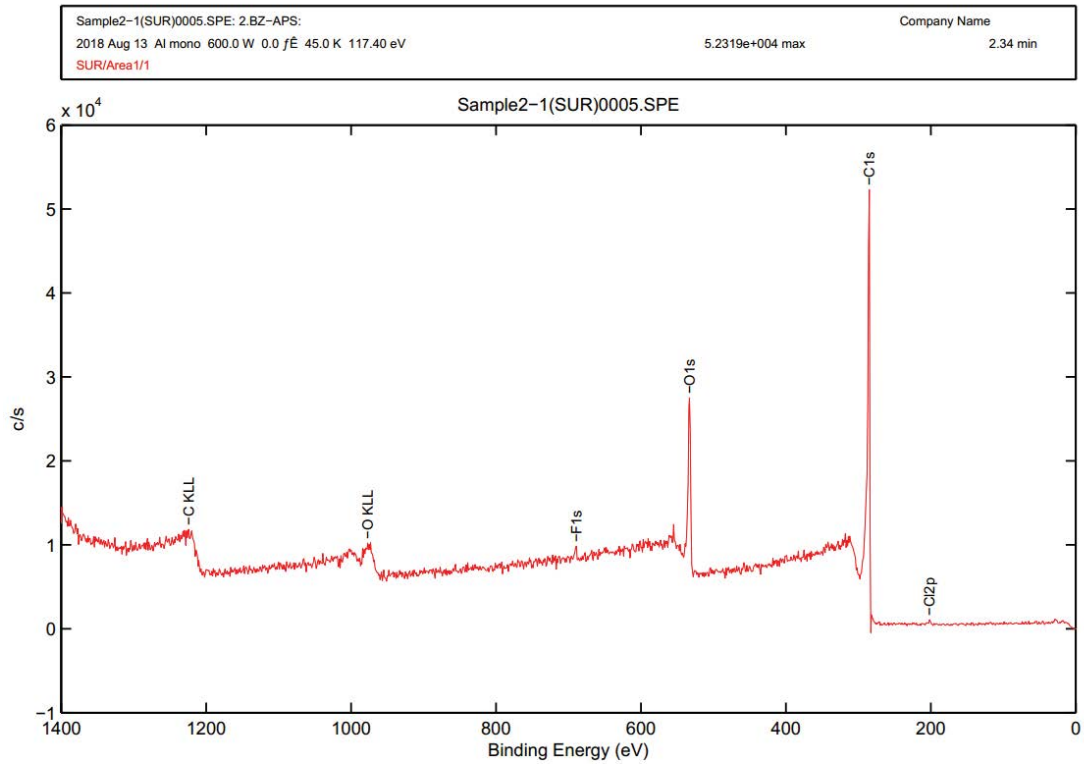

Fig. S1. Comparison of wide XPS spectra (a) XPS spectra of BZ and (b) XPS spectra of BZ-APS24h..